Compact Modeling of Threshold Voltage in Double-Gate MOSFET including quantum mechanical and short channel effects

K. Nehari[*], D. Munteanu[*], J.L. Autran[*,**], S. Harrison [*,***], O. Tintori[*], T. Skotnicki[***]

[*] Laboratory for Materials and Microelectronics of Provence (L2MP)
49 rue Joliot-Curie 13384 Marseille France, munteanu@newsup.univ-mrs.fr
[**]also with Institut Universitaire de France
[***] STMicroelectronics, 850 rue J. Monnet, 38926 Crolles France

ABSTRACT

A compact model for the threshold voltage in Double-Gate MOSFET is developed. The model takes into account short-channel effects, carrier quantization and temperature dependence of the threshold voltage. We assume a parabolic variation of the potential with the vertical position in the silicon film at threshold. An analytical expression for the surface potential dependence as a function of bias and position in the silicon film is also developed and used for the inversion charge calculation. The model is fully validated by 2D quantum numerical simulation and is used to predict the threshold voltage roll-off in Double-Gate MOSFET with very short channel lengths and thin films. The comparison with measured threshold voltage shows that the model reproduces with an excellent accuracy the experimental data. The model can be directly implemented in a circuit simulator code and used for the simulation of elementary Double-Gate MOSFET based-circuits.

Keywords: compact modeling, threshold voltage, Double-Gate MOSFET, short-channel effects, quantum effects

1 INTRODUCTION

Compact modeling of Double-Gate MOSFET incites very much interest presently, since Double-Gate structure is considered to be one of the best candidates for the MOSFET integration at the end-of-roadmap [1-2]. The aim of this work is to develop a short-channel quantum mechanical compact model for the threshold voltage (V_T) based on the decoupled 1D Poisson and Schrödinger equations in the silicon film. Recently, we have proposed an analytical V_T model for long channel devices including quantum effects and applying to both symmetric and asymmetric device [3]. This model is enhanced here for taking into account short channel effects and temperature dependence of V_T. The model is completely validated using a full 2-D quantum mechanical numerical simulation code [4] and is compared with experimental data extracted from Double-Gate devices fabricated using the SON process [5]. We present here the model development in the case of a symmetric Double-Gate device, but it can be very easily adapted to any asymmetric Double-Gate device (different oxides thicknesses or gate work-functions).

2 THRESHOLD VOLTAGE DEFINITION

Figure 1a shows the schematic of a symmetric Double-Gate and the variation of the surface potential Ψ_s in a horizontal cross-section in the channel (Figure 1b). A parabolic dependence for the potential at threshold in the vertical direction is assumed (Figure 1c):

$$\Psi(x,y) = \Psi_s(x) - \alpha(x) t_{Si} y + \alpha(x) y^2 \qquad (1)$$

where the calculation of $\alpha(x)$ is indicated in paragraph 4. The boundary conditions at the Si/SiO_2 interface are:

$$V_G - V_{FB} = \frac{\varepsilon_{Si}}{\varepsilon_{ox}} t_{ox}\xi_s + \Psi_s + \phi_F \qquad (2)$$

where Ψ_S and ξ_S are the potential and, respectively, the electric field at the interface. Potential Ψ and the charge (depletion charge and mobile charge) in the Si film are linked via the Poisson equation:

$$\frac{d^2\Psi}{dy^2} = \frac{qN_A}{\varepsilon_{Si}} + \frac{q}{\varepsilon_{Si}} n_i \, exp\left(\frac{q\Psi}{kT}\right) \qquad (3)$$

For defining V_T, it is important to remind that in Double-Gate MOSFET the usual definition of the V_T as the gate voltage where Ψ_s is $2\phi_F$ does no more apply [6]. Therefore, we define here V_T as the gate voltage for which the inversion charge, Q_{inv}, reaches a constant value:

$$Q_T = \frac{kT}{q} C_{ox} \qquad (4)$$

3 QUANTUM EFFECTS

The inversion Q_{inv} is quantum-mechanically evaluated using the following expression:

$$Q_{inv} = \frac{qkT}{\pi\hbar^2} \sum_{l,t} \sum_i m_{2D}^{t,l} g_{t,l} \, ln\left[1 + exp\left(-\beta\left(\tilde{E}_{l,t}^i + \frac{E_g}{2} - \psi_S(x_m)\right)\right)\right] \qquad (5)$$

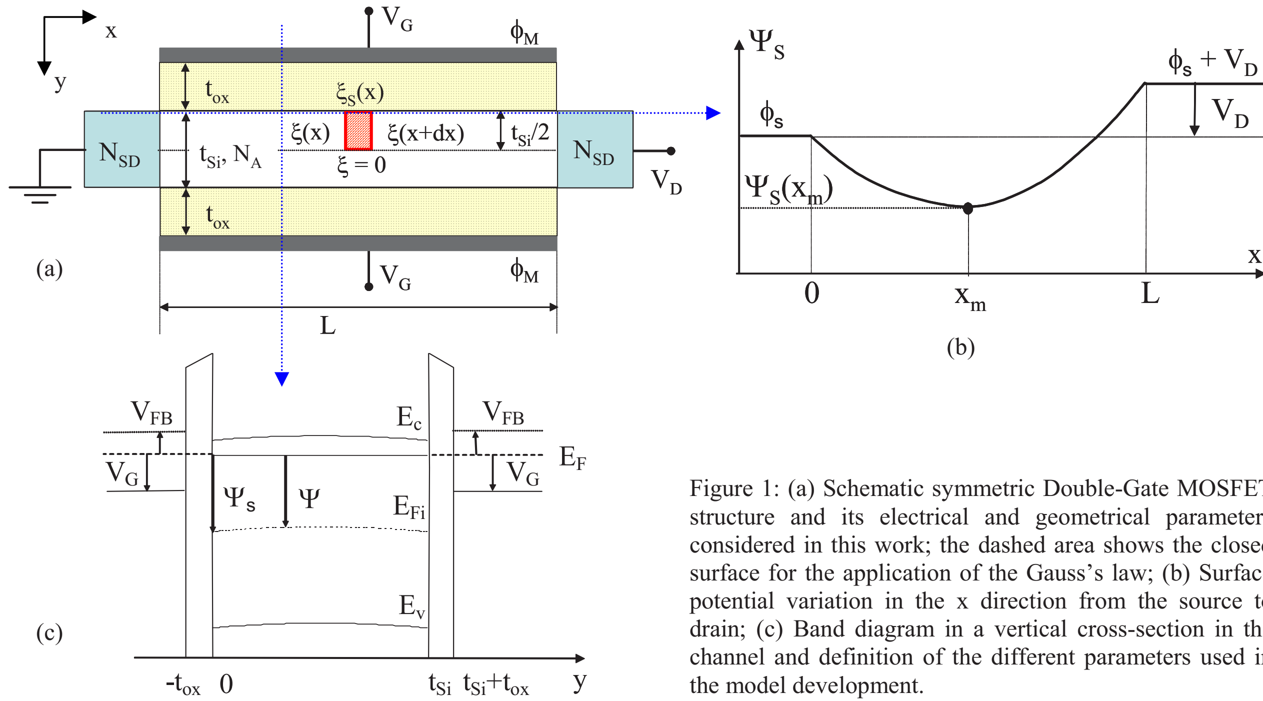

Figure 1: (a) Schematic symmetric Double-Gate MOSFET structure and its electrical and geometrical parameters considered in this work; the dashed area shows the closed surface for the application of the Gauss's law; (b) Surface potential variation in the x direction from the source to drain; (c) Band diagram in a vertical cross-section in the channel and definition of the different parameters used in the model development.

where $m_{2D}^{l} = m_{t}^{*}$, $m_{2D}^{t} = \sqrt{m_{l}^{*} m_{t}^{*}}$, $m_t^*=0.19\times m_0$, $m_l^*=0.98\times m_0$, $g_l=2$, $g_t=4$, $\beta=q/kT$.

In equation (5) $\Psi_s(x_m)$ is the minimum of the surface potential in the horizontal direction (Figure 1b) in the channel and $\tilde{E}^i_{l,t}$ are the energy levels. For calculating $\tilde{E}^i_{l,t}$ we consider in a first approximation that the band diagram in symmetric Double-Gate structure is close to an infinite rectangular well. The energy levels are then given by:

$$E^{i}_{l,t} = \frac{\hbar^2 \pi^2 i^2}{2 q m^{*}_{l,t} t_{Si}^2} \qquad (6)$$

In a second step, a more carefully evaluation of these energy levels can be performed using a standard method for first-order perturbation [3]. Considering the parabolic nature of the potential profile in the Si film, as described by equation (1), the first-order correction to apply to the energy levels in the well is given by:

$$\Delta E^{i} = \left\langle \varphi^{i} \middle| H \middle| \varphi^{i} \right\rangle \qquad (7)$$

where $H=-q(-\alpha t_{Si} y+\alpha y^2)$ is the Hamiltonian of the perturbation and ϕ^i are the electron wave functions associated to energy levels $E^i_{l,t}$. Finally, the first-order corrected energy levels are given by:

$$\tilde{E}^{i}_{l,t} = E^{i}_{l,t} + \Delta E^{i} \qquad (8)$$

Due to the analytical character of both ϕ^i and H, an elementary calculation gives ΔE^i in the case of an infinite rectangular well subjected to the considered perturbation:

$$\Delta E^{i} = \frac{\alpha t_{Si}^2}{6}\left[1 + \frac{3}{\pi^2 i^2}\right] \qquad (9)$$

Finally, the corrected energy levels are given by the following equation:

$$\tilde{E}^{i}_{l,t} = \frac{\hbar^2 \pi^2 i^2}{2 q m^{*}_{l,t} t_{Si}^2} + \frac{\alpha\, t_{Si}^2}{6}\left[1 + \frac{3}{\pi^2 i^2}\right] \qquad (10)$$

4 SHORT CHANNEL EFFECTS

For evaluating the inversion charge (relation (5)), the minimum of the surface potential, $\Psi_s(x_m)$, has to be calculated. For this purpose, the Gauss's law is applied to the particular closed surface shown in Figure 1a:

$$-\xi(x)\frac{t_{Si}}{2} + \xi(x+dx)\frac{t_{Si}}{2} - \xi_S(x)dx = -\frac{q N_A t_{Si}}{2\varepsilon_{Si}} \qquad (11)$$

The electric field $\xi(x)$ can be approximated by:

$$\xi(x) \approx -\frac{1}{\eta}\frac{d\psi_s(x)}{dx} \qquad (12)$$

NSTI-Nanotech 2005, www.nsti.org, ISBN 0-9767985-3-0 WCM, 2005

where η is a fitting parameter which incorporates the effects of the variation of the lateral field in the depleted film under the channel [7-8]. As demonstrated in [7], η is lower than 1 for $V_G=V_T$ and depends on the channel doping and thickness. Therefore this parameter has to be calibrated for each particular technology. After some algebraic manipulations and using (2) the following differential equation is obtained for the surface potential

$$\frac{d^2\psi_s}{dx^2}-\frac{2\eta C_{ox}}{\varepsilon_{Si}t_{Si}}\psi_s=\frac{\eta}{\varepsilon_{Si}t_{Si}}\left[qN_At_{Si}-2C_{ox}(V_{GS}-V_{FB}-\phi_F)\right] \tag{13}$$

The analytical solution of equation (9) is given by:

$$\psi_s(x)=C_1\exp(m_1x)+C_2\exp(-m_1x)-\frac{R}{m_1^2} \tag{14}$$

with coefficients C_1, C_2, m_1 and R given by

$$C_1=\frac{\phi_S[1-\exp(-m_1L)]+V_D+R\dfrac{1-\exp(-m_1L)}{m_1{}^2}}{2\sinh(m_1L)} \tag{15}$$

$$C_2=-\frac{\phi_S[1-\exp(m_1L)]+V_D+R\dfrac{1-\exp(m_1L)}{m_1{}^2}}{2\sinh(m_1L)} \tag{16}$$

$$R=\eta\frac{qN_At_{Si}-2C_{ox}(V_G-V_{FB}-\phi_F)}{\varepsilon_{Si}t_{Si}} \tag{17}$$

$$m_1=\sqrt{\frac{2\eta C_{ox}}{\varepsilon_{Si}t_{Si}}}\ ,\ \phi_S=(kT/q)\ln\left(N_AN_{SD}/n_i^2\right) \tag{18}$$

Combining (1), (2), (14) and (3), the expression of the parameter α(x) is easily obtained and then used for calculating $\tilde{E}^i_{l,t}$ (relation (10)).

The position in the channel, x_m, where Ψ_s reaches the minimum value is the solution of $d\Psi_s/dx=0$:

$$x_m=\frac{1}{2m_1}\ln\left(\frac{C_2}{C_1}\right) \tag{19}$$

Therefore, we obtain the following relation for $\Psi_s(x_m)$:

$$\psi_s(x_m)=2\sqrt{C_1C_2}-\frac{R}{m_1^2} \tag{20}$$

Finally, V_T is calculated by numerically solving the relation $Q_{inv}=Q_T$, where Q_{inv} is given by relation (5) (using (10) and (20)) and Q_T is given by (4).

5 MODEL VALIDATION

The model was validated by an extensive comparison with quantum numerical simulation using a full 2-D Poisson-Schrödinger code [4].

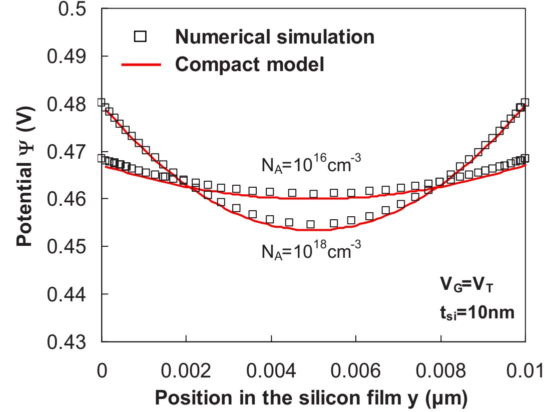

Figure 2: Variation of the potential as predicted by the compact model and comparison with numerical simulation.

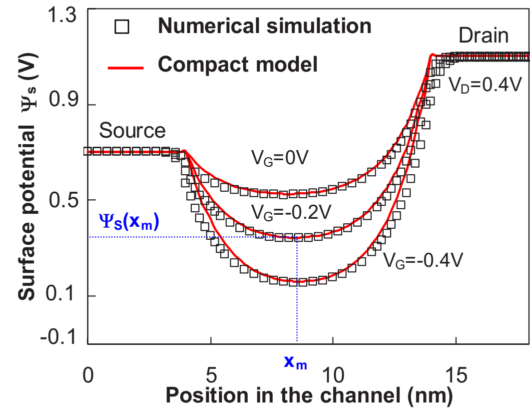

Figure 3: Ψ_s variation calculated with the analytical model (relation 14) and comparison with the 2D numerical code.

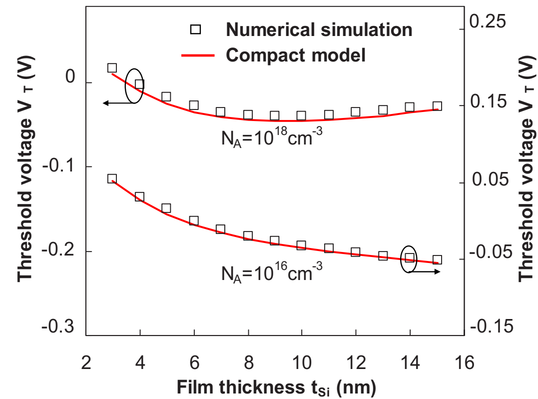

Figure 4: Comparison between V_T given by the compact model and quantum numerical simulation in long channel Double-Gate device with low and high channel doping.

In a first step, expressions (15) and (16), as well as the assumption of a vertical parabolic dependence of the potential in the film have been verified: as shown in Figures 2 and 3, the model fits very well the numerical data. In a second step, the threshold voltage model has been completely validated by numerical simulation. Figure 4 shows an example of this validation step on a long channel Double-Gate: very good match is obtained between compact model and numerical results for all film thicknesses and at low and high doping.

6 COMPARISON WITH EXPERIMENTAL DATA

Finally, the model was used to fit threshold voltage extracted on Double-Gate devices fabricated by SON process, as described in [5]. Devices with different film thicknesses (Table I) have been measured and the threshold voltage has been extracted from the $I_D(V_G)$ characteristics. As illustrated in Figure 5, the match between experiment and model is very satisfactory, showing that the model reproduces well the threshold voltage roll-off of the measured devices. Parameter η, which has been calibrated for each film thickness (Table I), is less than 1 but increases when the film thickness decreases (because the variation of the lateral field in the film becomes less accentuated) and is even equal to 1 for the thinnest film (10nm).

Device	t_{Si} (nm)	t_{ox} (Å)	N_A (cm^{-3})	η
A	30	20	~ 4×10^{18}	0.17
B	20	20	~ 4×10^{18}	0.5
C	15	15	~ 3.7×10^{18}	0.6
D	10	15	~ 2.5×10^{18}	1

Table I: Geometrical parameters of measured devices.

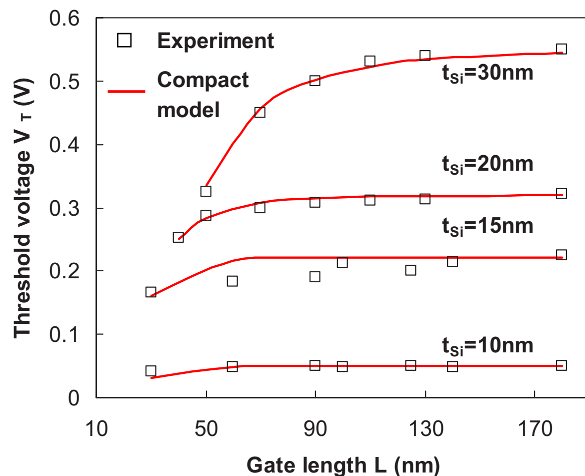

Figure 5: Comparison between measured V_T and 2-D quantum V_T calculated using the compact model.

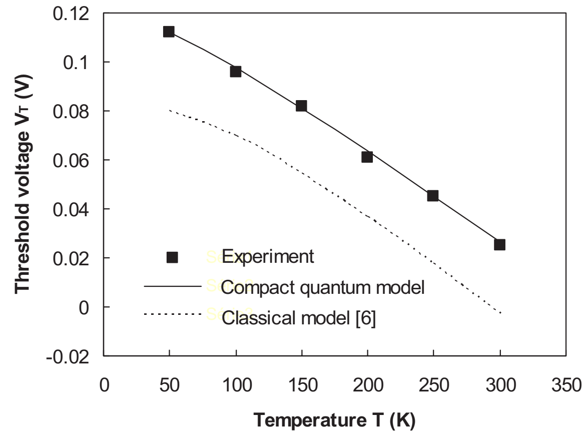

Figure 6: Fit of compact model on measured V_T on a long channel device at low temperature (t_{Si}=10nm, V_D=0.1V).

Moreover, the compact model has been successfully extended in low temperature simply using an appropriate model for the temperature dependence of n_i, the effective density of states in both conduction and valence band and the energy bandgap [9]. Figure 6 shows the remarkable fit on measured threshold voltage in a long channel Double-Gate device down to 50K.

7 CONCLUSION

A new compact model for the threshold voltage in symmetric Double-Gate devices has been developed. The model takes into account short-channel effects and quantum confinement of carriers in the direction perpendicular to the channel. The expression of the surface potential as a function of gate and drain biases and of the position in the channel has been developed and integrated in the calculation of the inversion charge. A very satisfactory concordance has been found between the threshold voltage calculated by the compact model and numerical data obtained with a 2D quantum numerical simulation code. Finally, we show that the model provides a very good prediction of the threshold voltage in real devices with different channel thicknesses and gate lengths.

REFERENCES

[1] D.J. Frank *et al.*, IEDM Tech. Dig., 553 (1992).
[2] Y. Taur, IEEE Trans. Electron Dev. **48**, 2861 (2001).
[3] J.L. Autran *et al.*, Proc. MSM/WCM, 163 (2004).
[4] D. Munteanu, J.L Autran, Solid State Electron. **47**, 1219 (2003).
[5] S. Harrison *et al.*, Proc. ESSDERC, 373 (2004).
[6] D.Munteanu *et al.*, Proc. ULIS, p. 35 (2003).
[7] S.Banna *et al.*, IEEE Trans. Electron Dev. **42**, 1949 (1995).
[8] S.Biesemans *et al.*, Solid-State Electron. **39**, 43 (1996).
[9] R.Vankemmel *et al.*, Solid State Electron. **36**, 1379 (1993).